

# Metastability exchange optical pumping low field polarizer for lung magnetic resonance imaging

GUILHEM COLLIER<sup>1\*</sup>, MATEUSZ SUCHANEK<sup>3</sup>, ANNA WOJNA<sup>1</sup>, KATARZYNA CIESLAR<sup>4</sup>,  
TADEUSZ PALASZ<sup>1</sup>, BARTOSZ GLOWACZ<sup>1</sup>, ZBIGNIEW OLEJNICZAK<sup>2</sup>, TOMASZ DOHNALIK<sup>1</sup>

<sup>1</sup>Institute of Physics, Jagiellonian University,  
Reymonta 4, 30-059 Kraków, Poland

<sup>2</sup>Institute of Nuclear Physics, Polish Academy of Sciences,  
Radzikowskiego 152, 31-342 Kraków, Poland

<sup>3</sup>Department of Chemistry and Physics, Agricultural University,  
al. Mickiewicza 21, 31-120 Kraków, Poland

<sup>4</sup>Université de Lyon, CREATIS-LRMN, CNRS,  
UMR5220, INSERM U630, Villeurbanne, France

\*Corresponding author: guilhem.collier@gmail.com

An extensive improvement of our low field polarizer is described. It produces <sup>3</sup>He gas polarized up to 40% in a 6 h decay time storage cell. Production rate was raised by a factor of 10 to 4–5 scc/min<sup>1</sup> thanks to the implementation of a new 10 W laser and a new design of a peristaltic compressor, easier to handle. Some applications of polarized gas are also presented: dynamic images of gas inhalation in the rat as well as a static image of human lungs using hyperpolarized gas were obtained.

Keywords: optical pumping, <sup>3</sup>He, table-top polarizer, magnetic resonance imaging (MRI) of the lungs.

## 1. Introduction

Despite its relative scarcity, hyperpolarized <sup>3</sup>He has become an important alternative tool to study the lung functions. In the last decade, magnetic resonance imaging (MRI) using <sup>3</sup>He has been successfully implemented in clinical research of asthma, cystic fibrosis, emphysema and lung cancer allowing one to perform well resolved ventilation

---

<sup>1</sup>scc is an acronym for standard cubic centimeter, corresponding to the number of atoms included in one mL (cubic centimeter) for a gas at atmospheric pressure (1013 mbar) and normal temperature (273.15 K).

and dynamic imaging, diffusion measurement and regional oxygen uptake assessment [1]. The main interest in  $^3\text{He}$  for lung imaging is its property of being a high contrast agent once it has been hyperpolarized. Indeed, a high nuclear polarization of  $^3\text{He}$  gas can be obtained by the metastability exchange optical pumping (MEOP) method. It consists of two steps. First, the optical pumping of the  $2^3S-2^3P$  transition (see notation in [2]) is performed, using circularly polarized laser light at 1083 nm, in the presence of a radio-frequency (rf) discharge, ensuring sufficient density of metastable atoms. A high electronic polarization of metastable atoms is transferred to nuclei by the hyperfine interaction. In the second step, the collisions of helium atoms in the metastable state and in the ground state lead to the transfer of nuclear polarization to helium atoms in the ground state.

The method was demonstrated for the first time in [3] and a detailed microscopic model for the MEOP was developed in [4]. In the standard operating conditions a low magnetic field, of the order of a few mT, plays the role of the guiding field for the nuclear polarization, and a low  $^3\text{He}$  gas pressure, of the order of a few mbar is used. In most favorable conditions, the nuclear polarization achieved can exceed 80% [5]. In practice, achieving a good polarization level and production of  $^3\text{He}$  usable in MRI is far from being straightforward. Regarding MEOP technique, different strategies of gas production have been established. A global and central massive production has been chosen in Mainz [6]. This group has designed an advanced bulky polarizer reaching an efficient gas production of 20 scc/min with a nuclear polarization of 75%. The disadvantages, however, are the high price due to the non-magnetic titanium alloy compressor driven by a hydraulic system, the big size of the polarizer containing five optical pumping cells of 2.4 m for a total volume of 36 L, as well as difficulties in adjusting to user demands with regard to gas shipment over large distances.

Another approach is to design smaller polarizers [7–10], easy to handle, storable and placed close to the MRI system for on-site production. Such polarizer has the advantage of having lower cost and less constraints but usually only allows one to reach lower polarisation level and much lower throughput than the system in Mainz. A similar table-top polarizer was designed a few years ago by our group [10], but typically had throughput of only 0.4 scc/min for an estimated final polarization of only few percent when extracted into a syringe. We present in this paper an extensive upgrade of this polarizer, whose main novelties are a new 10 W laser and a new design of a peristaltic compressor, which different groups have always been attempting to improve.

In Section 2, all the different modifications of the polarizer are listed. We then describe briefly the MRI facilities used for our applications in Section 3. In the last section, results are presented and discussed.

## 2. Low-field polarizer

In Figure 1, a general design of our table-top polarizer is schematically described and a picture of it is presented in Fig. 2. The main framework and the coils frame were

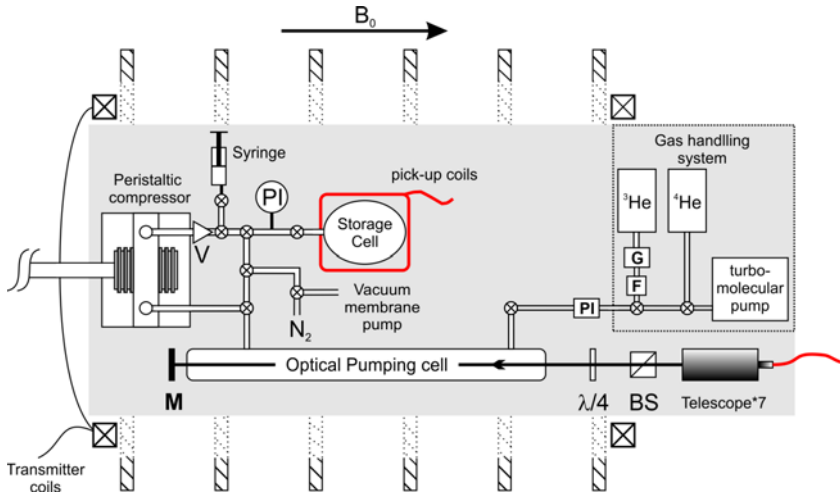


Fig. 1. Scheme of the table-top polarizer (see text). Six coils (cross-section) produce a homogeneous magnetic field. A gas handling system located under a 12 mm aluminium plate (G: getter, F: 50  $\mu\text{m}$  filter) deliver gas to the optical pumping cell where it is being polarized by a laser tuned at 1083 nm (BS: polarizing beam splitter). The gas is then compressed to a storage cell (V: one-way valve, PI: pressure sensor) with a peristaltic compressor. The same gas can be compressed a second time to atmospheric pressure inside a syringe for rat lung experiment using a bypass between the input and output of the compressor.



Fig. 2. Picture of the low field polarizer.

copied from the Protolab polarizer made in Paris [7, 8]. The supporting frame is made of fifteen square aluminium profiles of 6 cm in width inside which a main 12 mm thick aluminium plate is mounted. Wheels were added on the bottom of the framework, allowing an easy handling and transportation of the polarizer. The gas handling system was built inside a separate rectangular cuboid frame made of aluminium and Plexiglas. MEOP efficiency being strongly dependent of the gas purity, a particular care was taken to keep all the system airtight. All necessary needle valves (4172G6Y/MM by Hoke, Spartanburg, SC, USA) were helium leak-tight certified, and connection between the different elements was made using a 6 mm OD electropolished non-magnetic 316/316L stainless steel (Swagelok, Solon, Ohio, USA). The gas handling system is composed of a turbomolecular pump that can achieve a vacuum of  $10^{-8}$  mbar and a bottle of  $^4\text{He}$  for cleaning purposes of the optical pumping cell. The 1 L  $^3\text{He}$  bottle at a pressure of 15 bar (Spectra Gases Inc., Stewartville, New Jersey, USA) has a purity of 99.999% but for further cleaning, the gas passes through a PS2-GC50 SAES Getters S.p.A. (Lainate, Italy) getter, and an additional mechanical porous 0.5  $\mu\text{m}$  filter. A pressure sensor (24PC, Honeywell, Morristown, New Jersey, USA) was mounted at the output of it to control the pressure inside the optical pumping cell. Connection between gas handling system and the optical pumping cell is made using a flexible pipe from the CT convoluted metal tubing series and a glass metal connection (G304-4-GM3, Cajon Co, Solon, Ohio, USA). All the gas handling system fits inside a 40×60×90 cm cage that can be placed under the main plate of the polarizer. The actual dimensions of the main framework plus gas handling system are 70×160×170 cm and make it easily transportable to any MRI facility.

## 2.1. Guiding field

A guiding field of 16.4 gauss is produced by 3 pairs of square coils of 20 cm side. The frame of the coils is made of 2 mm thick aluminium whose cross-section has an open square shape. Grooves of the 2 inner pairs of coils have a 14 mm thickness and 22 mm for the external ones. Positions and number of turns for each coil were optimized by a Matlab program, taking into account the different filling height of the groove depending on the number of turns of a 0.8 mm diameter copper wire. To be more realistic, the filled groove was not assimilated to one loop of current but discretized into nine equally spaced loops centered around the center of the groove.

An optimized configuration was found to be 85, 100 and 225 turns respectively for the 6, 19.1 and 36.8 cm distances from the center of symmetry of the system (see Fig. 3). The simulations were experimentally verified with a three axis MAG-03 MS fluxgate magnetometer (Bartington Instruments Ltd, Witney, Oxfordshire, United Kingdom). The power supply of the probe was home made and gave a precision of 0.01%. The probe was mounted on a Plexiglas structure that allowed investigation of a matrix of 3.5 cm steps along transverse direction and it was manually moved with a step of 1 cm along the magnetic field direction. The experimental results gave a good agreement with the simulation and a final homogeneity of 0.15% was obtained in the location of a cylindrical optical pumping cell 48 cm long, 0.01% for a 100 mL

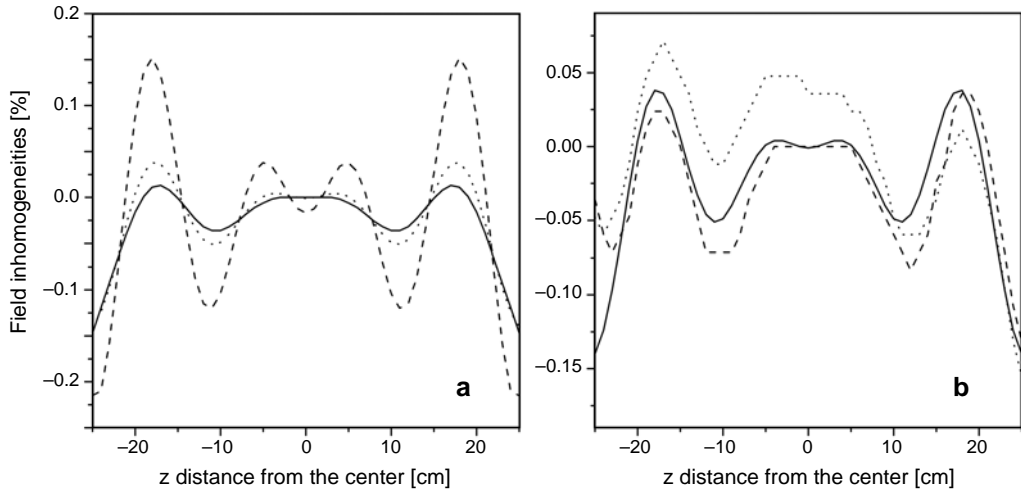


Fig. 3. Computation and experimental data of the magnetic guiding field deviation ( $1000 \times \Delta B/B$ ) inside the set of 6 square coils. The magnetic field is along the  $z$  direction. **a** – Matlab computation of our magnetic field inhomogeneities for three different distances from the symmetric axis of the square frames (solid line, dotted line and dashed line are respectively 0, 3.5 and 7 cm from the axis in the diagonal direction of the square frame). **b** – Comparison between computed (solid line) and experimental values (dotted and dashed lines) measured with a Bartington magnetometer. The dotted line corresponds to the left side of the axis where the 48 cm long optical pumping cell is lying and the dashed line to the right side where the NMR and the 100 mL, 5 cm long storage cell is located.

storage cell which serves to perform the NMR measurement, and 0.06% for the second NMR system dedicated to a 1.1 L storage cell.

## 2.2. Laser

The 50 mW DBR diode laser was replaced by a new ytterbium 10 W doped fiber laser (2.1 GHz FWHM, CUS-BT-YFL-1083-HE-100-COL, Keopsys, Lannion, France) with the same wavelength of 1083 nm. An APC collimator (model F220APC, Thorlabs, Newton, New Jersey, USA), coated for 1064 nm with a focus length of 11.17 mm was mounted directly on the output of the fiber. To improve efficiency of optical pumping inside the 5 cm diameter optical pumping cell, the beam was expanded by a Kepler-like telescope  $F2/F1 = 7$  (EKSMA OPTICS, Vilnius, Lithuania). The final full width at half maximum of the Gaussian beam profile was 4.9 mm. The beam was circularly polarized with a 5 cm cube polarizing beam splitter and a multiple order plate with  $\lambda/4$  retardation. The beam was back-reflected by a dielectric mirror after first passage through the cell to double the efficiency.

## 2.3. Optical pumping cell

Thanks to the new guiding field, a new longer Pyrex optical pumping cell of 48 cm in length, 5 cm in diameter with optical windows have been implemented. Apiezon L grease was used for lubrication of input and output valves. Some 5 cm glass capillaries

of 1.8 mm in diameter were located at the input and output of the cell to constraint the gas flowing in one direction only and keep impurities out of the storage cell and gas handling system. The cell was located 3.5 cm off the center of the coils symmetry axis.

## 2.4. Storage cell and gas transportation

To store the polarized  $^3\text{He}$  after compression, three different storage cells were used. A small 100 mL Pyrex cell was dedicated to short rat lung imaging experiments in our 0.088 T permanent magnet based system and optical calibration of the NMR signal. This cell was previously demagnetized [11]. Following this procedure, a decay time of 54 min was measured by NMR. A 500 mL quartz cell with a longer decay time of 4 h was used to store larger quantities of helium for longer experiments. Thanks to a bypass system implemented between the output and the input of the peristaltic compressor (see Fig. 1) a portion of the gas can be compressed a second time to atmospheric pressure into a 12 mL syringe. This latter is used to transfer  $^3\text{He}$  from the low field polarizer to the low-field MRI system located 10 m away in our laboratory. Previously polarized  $^3\text{He}$  was mixed in the storage cell with a buffer gas ( $^4\text{He}$  or  $\text{N}_2$ ) to reach a pressure higher than 1 atm and only a small amount of  $^3\text{He}$  was retrieved by distending the mixture inside a plastic syringe. This new process of extracting helium avoids losses due to gas mixing and shows a factor of 3 increase in total magnetization inside the syringe. Losses due to the first and the second compression inside the peristaltic compressor and also during transportation in the presence of a non-homogeneous magnetic field are difficult to accurately assess but the relaxation time of  $^3\text{He}$  inside the syringe in the low-field MRI system was measured to be longer than 3 min (see Fig. 4).

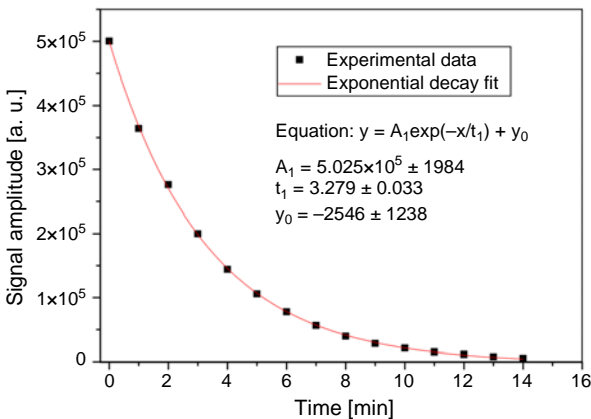


Fig. 4. Relaxation of magnetization inside a 12 mL polypropylene/polyethylene syringe in our 0.088 T permanent magnet. Plastic syringe was used to transport polarized  $^3\text{He}$  from the storage cell to the scanner and to inflate lungs of the tracheotomised rat. Time before application was reduced as much as possible and kept below 20 s, which is equivalent to a total magnetization loss lower than 10%.



Fig. 5. Transport box and vessels from Mainz University group for  $^3\text{He}$  storage during journey to hospital.

For human lung experiments, storage cells of 1.1 L volume were bought together with a magnetic transport box (Fig. 5) from Arbeitsgruppe Helium-3, Institut für Physik, Universität Mainz [12]. As was shown in [13] that short relaxation times could be attributed to ferromagnetic contaminants, the vessels were made by Schott AG (Mainz, Germany) from a special aluminosilicate-glass containing a minimum of these paramagnetic centers and the best flask was certified to have a 150 h wall relaxation time. In practice, our gas handling system at the output of the compressor being not as clean as it is at the input of the OP cell, an additional relaxation due to impurities shortened this time. The NMR measurement gave a decay time of polarization inside the cell of 6 h. To store and keep the vessels inside a magnetic homogeneous guiding field, the transport box is magnetically shielded with permanent magnet and pieces of mu-metal. It produces a field of 10 gauss with relative gradients lower than  $10^{-3} \text{ cm}^{-1}$ . This gives a relaxation time due to gradient inhomogeneities close to 150 h at 1 bar. Once in the hospital and the preliminary calibrations on patient executed, the transport box was placed close to the end of the fringe field of the scanner. After opening the box, gas was extracted into a 1 L Tedlar gas sampling bag (model GST001S-0707, Jensen Inert Products, Coral Springs, Florida, USA) using a similar design of the peristaltic compressor as the one used in the table-top polarizer. The sample bag was pre-filled with 100 mL of nitrogen to avoid too fast a relaxation with its inner surface during the beginning of helium compression. After a first rinse of the lungs with nitrogen, gas mixture was directly administrated to the volunteer through the sample bag. Delay between the end of  $^3\text{He}$  polarization and the time of the scan was approximately 1.5 h, including 45 min of transportation.

## 2.5. Peristaltic compressor

To replace the peristaltic compressor borrowed from the Kastler Brossel Laboratory [14], a new transparent design was developed, tested and experimentally approved (see



Fig. 6. Picture of the new peristaltic compressor design.

Fig. 6). The compressor is built of the following fixed elements: the main body made of polycarbonate, two Plexiglas lids with bearing shells, Plexiglas pressing bar, radiators, peristaltic tube and Plexiglas oil chamber. The rotor of the compressor is made of polyamide and turns on the antimagnetic steel axis. The pressing polyamide rollers rotating on non-magnetic steel axis play the role of the compressor's valves. The main motivation for this new design was to facilitate the replacement of the inner peristaltic tube. The replacement procedure was then shortened from 30 min to 15 min. To lengthen the lifetime of the tube, inorganic oil was inserted inside the compressor and two radiators were mounted on both sides of the main body to dissipate the heat energy released during friction. To improve the flow circulation, a vacuum of the order of a few mbar was maintained by a rotary pump inside the body of the compressor, while operating. This vacuum prevents the tube from shrinking under atmospheric pressure while compressing helium that is polarized in the optical pumping cell at 2–3 mbar. A small gas reservoir is located between the compressor and the vacuum chamber to keep the oil inside the main body. Several peristaltic tubes from Masterflex (Cole-Parmer, Vernon Hills, Illinois, USA), models C-FLEX (50 A), Pharmed BPT, Norprene (A 60 G) and BioPharm Plus silicone have been tested, of which only the first two showed satisfactory parameters to be used inside the compressor. NMR measurements on the storage cell showed that both of them gave similar and reproducible polarization levels but for mechanical considerations the Pharmed tube was chosen due to a more rigid property, allowing for a longer lifetime up to 20 h. Compressors of two different sizes were produced. The first one with a similar core diameter of 8 cm as the older compressor was built to work with the Pharmed BPT tube model 06508-17, inside diameter of 6.4 mm. A larger model, core diameter of



9.5 cm and 12.7 mm 06508-82 tube model, was also tested to increase the production of polarized  $^3\text{He}$ .

## 2.6. Nuclear magnetic resonance (NMR)

The nuclear magnetic resonance (NMR) system was completely rebuilt (see Fig. 7). New square Helmholtz transmitter coils, of 107 cm radius, 20 turns each, were mounted on the main aluminium frame to give a homogeneous  $B_1$  field over the storage cells volume and an easy access to different elements. They have been tuned to 55 kHz (inductance  $L = 3.85$  mH, resistance  $R = 12.63 \Omega$ ). Radio-frequency pulse at a frequency of 53.3 kHz, is produced by a generator (GW Instek GFG 3015), whose external trigger option allows a precise control of the number of oscillations, and amplified with a 100 W DMOS audio amplifier (model TDA 7294). Concerning the pick-up coils, two different systems were built. The first one consists of two circular coils of 40 turns, 30 mm apart from each other ( $R = 24 \Omega$ ,  $L = 1.55$  mH) and whose diameter (72 mm) was chosen to fit the size of the 1.1 L storage cell. A smaller one was dedicated to a 5 cm long and 5 cm diameter storage cell and was made of two rectangular coils of 120 turns each ( $R = 50 \Omega$ ,  $L = 3.76$  mH). Litz wire was used for both pick-coils and each of them has their own tuning and matching circuits. A similar  $Q$  factor of 20–25 was achieved in both coils.

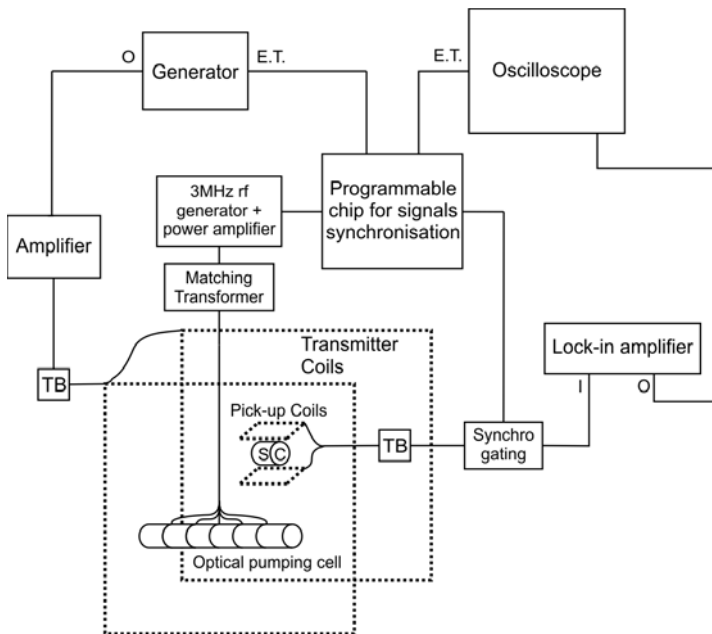


Fig. 7. Scheme of the NMR acquisition (see text). (TB: tuning and matching circuit, I: input, O: output, SC: storage cell, E.T.: external trigger). A microprocessor at the center of the NMR system is used to control the different elements.

During NMR experiment a chosen pulse was sent through transmitter coils that causes free precession of the storage cell magnetization. This free induction decay (FID) signal at 53.3 kHz was then detected by the pick-up coils and a digital lock-in amplifier (LIA, SR 830, Stanford Research Systems, Sunnyvale, California, USA) applied synchronous detection. The output of the lock-in amplifier was recorded on a numerical oscilloscope that had the possibility to transfer saved waveforms from its memory to a personal computer via USB connector. The free induction decay was revealed by the LIA using its internal clock a little off resonance to get a sufficient number of oscillations during the decay. Data analysis was performed on a standalone PC by performing a peak-to-peak analysis of the oscillations and fitting them to retrieve the initial amplitude of the FID. A proper gating circuit protects the LIA at the time of the rf pulse and turns off the discharge during data acquisition to minimize the noise. The key element of the NMR system is a programmable microprocessor (ATmega 8, Atmel, San Jose, California, USA) which is synchronizing all the different elements together. Four output signals are delivered by the microprocessor:

- one switches off the radio-frequency discharge inside the OP cell just before the rf pulse,
- a second signal is sent to the external trigger of the generator and commands the NMR pulse length,
- an opto-isolator coupled to flip flop diodes opens the gate and lets the signal go through to the LIA after the ringing time of the transmitter coils,
- a last logic signal triggers the acquisition of the oscilloscope.

It is possible to program the length of the pulse, the delay between two pulses, the ringing off time after the pulse and the acquisition time through a simple interface with display (LCD panel). This home made device therefore offers an easy control of all the parameters and facilitates the NMR acquisition.

At last, NMR was calibrated against an optical detection method [15, 16]. A sealed cell with the exact same shape as the 100 mL storage cell, filled with 1 torr of pure  $^3\text{He}$  was polarized inside the NMR system by the pump laser. The optical detection relies on the absorption of a longitudinal attenuated probe laser tuned at 1083 nm on  $C_9$  or  $C_8$  lines of  $^3\text{He}$ . Indeed, the ratio of absorption rates for positively and negatively polarized probe beam is directly related to the spin temperature distribution in metastable state and then to the nuclear polarization. This method is very accurate and does not depend on pressure. Knowing precisely the polarization and the total amount of  $^3\text{He}$  inside our sealed cell, nuclear magnetization inside the storage cell can be easily deduced.

### 3. MRI facilities

#### 3.1. Low field (0.088 T) scanner

The imaging of rat lungs was performed at a low field MRI scanner described in detail elsewhere [17]. It was specially designed for small animal lung imaging using polarized  $^3\text{He}$  gas. The scanner is based on a 0.088 T permanent magnet (AMAG,

Poland) equipped with a biplanar actively shielded gradient coils (30 mT/m, NRC, Winnipeg, Canada) controlled by commercial MR Research System (previously SIMS, Surrey, Great Britain) MR4200 Narrow Band console. Dual-frequency 2.84 MHz for  $^3\text{He}$  (alternatively 3.73 MHz for  $^1\text{H}$ ) solenoid coil was used for NMR signal detection.

For *in vivo* animal study three adult rats (race: Wistar, 400 g) were used. All experiments using animals were approved by national research ethics committees and conducted in accordance with Polish regulations and animal protection law. Each animal was anesthetized by intraperitoneal injection of chloral hydrate (40 mg/100 g body weight) and afterwards tracheotomized to simplify  $^3\text{He}$  gas injection. After each hour 1/3 of the anesthetic dose was injected again to prevent animal wake up. The animals were placed in a supine position on a home-built holder in the center of the rf coil. Just before imaging the volume of 7 mL of polarized  $^3\text{He}$  gas was introduced to the rats lung directly from the syringe via the trachea catheter.

For image acquisition we employed standard FLASH sequence (flip angle  $7^\circ$ , FOV = 80 mm,  $128 \times 128$  matrix, slice thickness 80 mm, sampling bandwidth 10 Hz, no averages, total acquisition time 1.6 s). Additionally, a radial sequence was developed for both static and dynamic imaging. The technique uses the following parameters: flip angle  $7^\circ$ , FOV = 80 mm, number of samples 128, total acquisition time 4 s and 20 s, for static and dynamic imaging, respectively. Both protocols utilized low-field excitation pulses optimal for polarized  $^3\text{He}$  imaging. The important advantage of radial sequence as compared to FLASH is that it allows performing dynamic imaging of gas inflow with a good temporal resolution, following a single gas injection.

### 3.2. Clinical 1.5 T scanner

The clinical experiments were performed at a Siemens Sonata scanner at 1.5 T (see Fig. 8) in collaboration with the team at the John Paul II Hospital in Kraków (Poland).



Fig. 8. Sonata scanner at the John Paul II Hospital with  $^3\text{He}$  coil from RAPID Biomedical. In the center of the coil, a first phantom (see text) is placed for angle calibration experiment.

A necessary update of the scanner's software and the purchase of a  $^3\text{He}$  birdcage lung coil from RAPID Biomedicals allowed us to perform  $^3\text{He}$  experiments at a frequency of 48.5 MHz. In order to test the system, a first phantom consisting of a 250 mL vessel filled with 1.363 bar of  $^3\text{He}$  and 440 mbar of  $\text{O}_2$  was realized. A similar phantom was used already in Orsay [18]. Only 14.02 mmol of thermally polarized  $^3\text{He}$  is sufficient to get an FID from the phantom and the oxygen is used to shorten the longitudinal relaxation time  $T_1$  [19].

Using a spectroscopic sequence from Siemens, adapted for multinuclear experiments, a  $T_1$  of 3.1 s was found and the flip angle calibrated. Gradient recalled echo sequences being the most commonly used sequences in MRI of hyperpolarized nuclei, a multinuclear multislice 2D spoiled gradient echo (SPGR) sequence, also known as fast low-angle shot (FLASH), was written and implemented on the scanner.

## 4. Results

### 4.1. $^3\text{He}$ production using the table-top polarizer

Thanks to all the improvements described above (optimized guiding field, new laser, optical pumping and storage cells, peristaltic compressor), the table-top polarizer is now able to work in a continuous mode. The new framework gives an easier open access to the elements inside and the possibility to transport the polarizer. The new calibrated NMR system gives the value of polarization inside the storage cell. The system was verified to give reproducible 30–40% of polarization for a pressure between 2.5 and 3 mbar inside OP cell during optical pumping. At this pressure and for a rotation speed of 4 to 5 Hz, the first design of peristaltic compressor has a production rate of 0.8–1 scc/min. The second larger version, working with a peristaltic tube of two times bigger diameter, also appeared to work satisfactorily and reaches 3.5–4 scc/min. As a reference, approximately 10 scc of gas are needed for a single rat lung experiment. Which means that within 3 min of compression the necessary volume of  $^3\text{He}$  can be polarized. For human experiment, the required volume is much higher: around 250–300 scc. This is obtained after about 1 h and 15 min of compression.

### 4.2. Small animal experiments

Preliminary tests were performed on a syringe phantom. The first test was made using a spectroscopy sequence to check the increase of total magnetization and compare this value to our previous experiments [10]. Results showed an increase of a factor of 7 in the total magnetization contained in a 10 mL syringe. The new way to extract the gas from the storage cell was responsible for an additional increase of a factor of 3, which means that new MRI experiments were possible with at least 20 times higher signal. New radial static and dynamic sequences were first implemented and tested with this phantom (Fig. 9). The static radial image is shown on the left. The 2 mm diameter nozzle and the 1 mm thick septum are well visible at the top and the bottom of

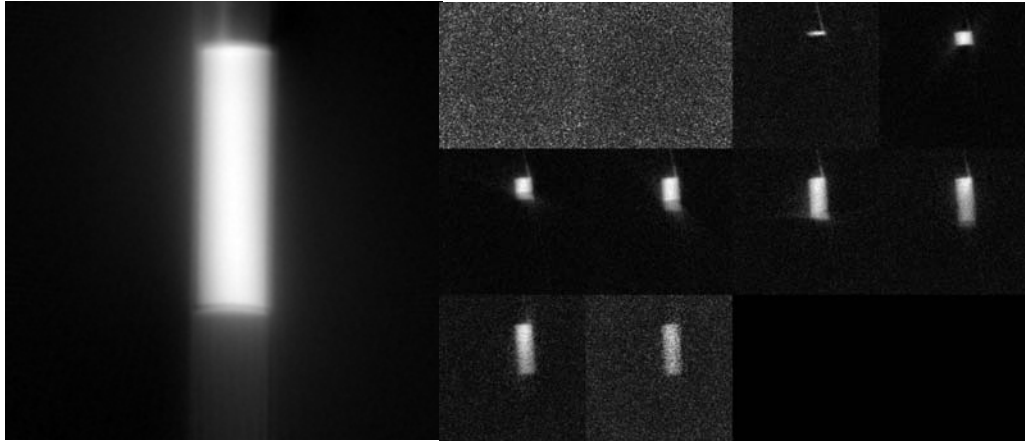


Fig. 9. Preliminary tests of the radial sequence made with a syringe phantom filled with  $^3\text{He}$  in a 0.088 T permanent scanner. Left: static radial 2D projection image acquired with 256 samples and 200 views, 10 cm field of view (FOV), 25 kHz bandwidth,  $6.1^\circ$  flip angle, acquisition time  $t_{\text{ac}}$  of 4 s, TR = 20 ms. Right: dynamic series of radial 2D projection sliding window images with 128 samples and 100 views, 10 cm FOV, 33 kHz bandwidth,  $8^\circ$  flip angle,  $t_{\text{ac}} = 21$  s.

the image, respectively. An artifact inherent to the radial reconstruction is responsible for the white vertical band pattern outside the syringe. On the right side of Fig. 9, a series of 10 images obtained using the projection sliding window sequence are presented. The sequence started before  $^3\text{He}$  entered the syringe, which explains the first 2 empty images of the series. The syringe was completely filled on the 8-th image. Then, total magnetization is decreasing due to the relaxation process and the rf pulsing. That is why the image SNR gradually decreases in the 9-th and 10-th image.

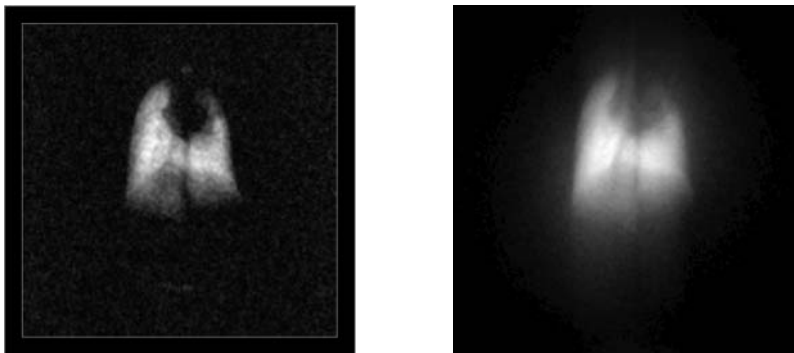


Fig. 10. Transverse  $^3\text{He}$  images of rat lungs *in vivo* acquired with the (left) FLASH sequence (slice thickness 80 mm, FOV = 80 mm,  $128 \times 128$  imaging matrix,  $8^\circ$  flip angle, 10 kHz bandwidth, no averaging, echo time = 7 ms, repetition time = 32 ms,  $t_{\text{ac}} = 4$  s) and the (right) projection radial one (FOV = 80 mm, 128 samples per 200 views, repetition time = 20 ms,  $t_{\text{ac}} = 4$  s, 10 kHz bandwidth, flip angle  $7^\circ$ , no averaging).

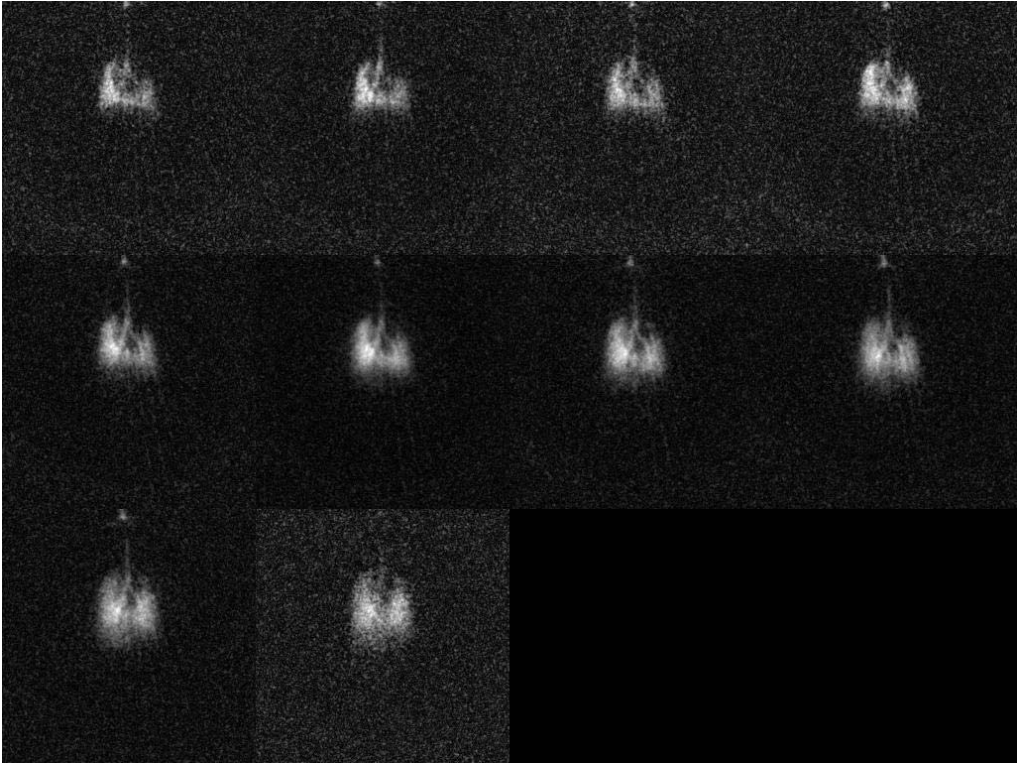


Fig. 11. Transverse  $^3\text{He}$  radial projection sliding window images of rat lungs *in vivo* (100 mm field of view, 128 samples and 100 views, 33 kHz bandwidth,  $8^\circ$  flip angle,  $t_{\text{ac}} = 20$  s).

These tests were followed by *in vivo* experiments with rats. Compared to the results previously reported by our group [17], a two-fold increase in spatial resolution and a four-fold increase in the SNR were observed, significantly improving the quality of the static images acquired during breath-hold (Fig. 10) as well as the dynamic images representing the gas inflow into the animal's lung (Fig. 11).

### 4.3. Human lung images

Preliminary tests were required to validate the sequence. The signal coming from the first phantom described in Section 3.2 being too low for an imaging sequence, we decided to optically pump a 11.5 cm long cell of 15 mm inner diameter filled with 128 mbar of  $^3\text{He}$  directly inside the scanner. The cell had a volume of approximately 20 mL, which corresponds to 2.5 scc but a polarization of the level of 30% can be obtained at 2 T. The different mechanisms and features of metastability exchange optical pumping in high field are not the subject of this article and are described elsewhere [20, 21]. A 500 mW laser was tuned at 1083 nm on the  $f^{2m}$  pumping line (see notation in [20]). After waiting a few minutes for the steady state polarization to be reached, the FLASH sequence was successfully tested with this phantom.

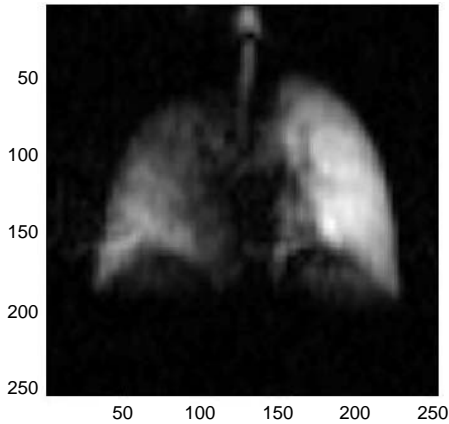


Fig. 12. Transverse  $^3\text{He}$  image of healthy volunteer's lungs using a FLASH sequence (20 cm slice thickness, 35 cm FOV,  $64 \times 64$  matrix,  $11^\circ$  flip angle, 16.64 kHz bandwidth, TE = 3.6 ms, TR = 7.5 ms).

Thanks to the new larger design of the peristaltic compressor, a few boluses of  $^3\text{He}$  could be carried to hospital inside the transport box and the storage cell. The polarization process takes 1 h to get 240 scc of  $^3\text{He}$ . The polarized gas was then mixed with  $\text{N}_2$  until reaching the atmospheric pressure inside the 1.1 L storage cell. Once in hospital, 81% of the total gas was extracted to the Tedlar bag previously rinsed with  $^4\text{He}$ . Lungs of a healthy volunteer were washed with 1 L of clean  $\text{N}_2$  before inhalation from the Tedlar bag. The image was taken 1 h after the end of the polarization process. The FLASH sequence was launched directly after inhalation. The field of view was  $35 \times 35$  cm for a  $64 \times 64$  matrix. A bandwidth of 16.64 kHz was used with a slice thickness of 20 cm to cover the whole lungs. There was no averaging and the sequence lasted approximately 500 ms (TE = 3.6 ms and TR = 7.5 ms). An  $11^\circ$  flip angle used in the experiment was calculated to be optimal [22]. The result is shown in Fig. 12. This image is the first MRI picture of human lungs using hyperpolarized gas made in Poland.

## 5. Conclusions

Improvements in our table-top polarizer, leading to the efficiency of 3.5–4 scc/min and a reproducible corresponding polarization of about 30–40% inside storage cell have been presented in this paper. The improvements are mainly due to the implementation of a broader bandwidth 10 W laser and a new design of the peristaltic compressor. Thanks to these modifications the magnetization was increased by a factor of 20, which allowed improved FLASH rat lungs pictures to be taken and moreover, to implement radial dynamic and static sequences. These ventilation images show a sufficient resolution and SNR to be used for diagnostic or medical tests. In addition we were also able to polarize a necessary quantity of  $^3\text{He}$  to take the first picture of human lungs made in Poland. Compared to rat images, the resolution of human lung

images is still low. A major issue for this problem is probably the loss of polarization during transportation and extraction. The losses due to relaxation time inside transport box and storage cell are minimal and can be easily assessed: the decay time is of the order of 6 h and the transport lasts 1 h (corresponding to 15% loss of magnetization), the losses due to the transfer of storage cell inside transport box were checked to be around 7%, only 81% of the gas mixture was compressed inside the Tedlar bag. But the main loss is probably due to the time spent (around 1.5 min) during compression inside the Tedlar bag in the non-homogeneous fringe field of the magnet. The transport of the bag inside the scanner is probably adding some losses. An easy solution to this problem would be to build a second smaller guiding field close to the magnet for minimizing the losses during the second compression. In the same way the table-top polarizer could be transported close to magnet in hospital and the gas directly produced few meters away from it.

But none of these solutions have been chosen by our group for future experiments. As evoked briefly earlier in Section 4.3, an alternative solution would be to perform MEOP at higher magnetic field and build a high field polarizer [23]. Previous promising experiments have been done and showed a great increase in production rate efficiency. This would solve both the problem of transportation and polarization time and will be tested in the near future.

*Acknowledgements* – We gratefully acknowledge Pierre-Jean Nacher from LKB in Paris for his support and advice. This work was partially supported by the Polish Ministry of Science and Higher Education (SPUB 547/6.PRUE/2008/07), the Marie Curie Research and Training Network PHeLINet (MRTN-CT-2006-036002) and the European Regional Development Fund under Operational Programme Innovative Economy Operational Program NLTK.

## References

- [1] KAUCZOR H.-U., *MRI of the Lung*, Springer, Heidelberg, 2009, pp. 36–56.
- [2] COLEGROVE F.D., SCHEARER L.D., WALTERS G.K., *Polarization of  $He^3$  by optical pumping*, Physical Review **132**(6), 1963, pp. 2561–2572.
- [3] WALTERS G.K., COLEGROVE F.D., SCHEARER L.D., *Nuclear polarization of  $He^3$  gas by metastability exchange with optically pumped metastable  $He^3$  atoms*, Physical Review Letters **8**(11), 1962, pp. 439–442.
- [4] NACHER P.J., LEDUC M., *Optical pumping in  $^3He$  with a laser*, Journal de Physique **46**(12), 1985, pp. 2057–2073.
- [5] STOLTZ E., MEYERHOFF M., BIGELOW N., LEDUC M., NACHER P.-J., TASTEVIN G., *High nuclear polarization in  $^3He$  and  $^3He$ - $^4He$  gas mixtures by optical pumping with a laser diode*, Applied Physics B **63**(6), 1996, pp. 629–633.
- [6] WOLF M., *Highest  $He$ -3 nuclear spin polarization production by metastable exchange pumping*, Dissertation zur Erlangung des Grades Doktor der Naturwissenschaften am Fachbereich Physik der Johannes Gutenberg-Universität in Mainz, 2004, available online: <http://ubm.opus.hbz-mrw.de/volltexte/2005/655/>.
- [7] NACHER P.-J., TASTEVIN G., MAITRE X., DOLLAT X., LEMAIRE B., OLEJNIK B., *A peristaltic compressor for hyperpolarized helium*, European Radiology **9**, 1999, article B18.



- [8] CHOUKEIFE J., MAITRE X., NACHER P.-J., TASTEVIN G., *On-site production of hyperpolarized helium-3 gas for lung MRI*, Proceedings of the 11th ISMRM Scientific Meeting and Exhibition, July 10–16, 2003, Toronto, Canada, p. 1391.
- [9] GENTILE T.R., RICH D.R., THOMSON A.K., SNOW W.M., JONES G.L., *Compressing spin-polarized  $^3\text{He}$  with a modified diaphragm pump*, Journal of Research of the National Institute of Standards and Technology **106**(4), 2001, pp. 709–729.
- [10] SUCHANEK K., CIESLAR K., OLEJNICZAK Z., PALASZ T., SUCHANEK M., DOHNAŁIK T., *Hyperpolarized  $^3\text{He}$  gas production by metastability exchange optical pumping for magnetic resonance imaging*, Optica Applicata **35**(2), 2005, pp. 263–276.
- [11] THIEL T., SCHNABEL A., KNAPPE-GRÜNEBERG S., STOLLFUß D., BURGHOFF M., *Demagnetization of magnetically shielded rooms*, Review of Scientific Instruments **78**(3), 2007, article 035106.
- [12] HIEBEL S., GROßMANN T., KISELEV D., SCHMIEDESKAMP J., GUSEV Y., HEIL W., KARPUK S., KRIMMER J., OTTEN E.W., SALHI Z., *Magnetized boxes for housing polarized spins in homogeneous fields*, Journal of Magnetic Resonance **204**(1), 2010, pp. 37–49.
- [13] SCHMIEDESKAMP J., ELMERS H.-J., HEIL W., OTTEN E.W., SOBOLEV YU., KILIAN W., RINNEBERG H., SANDER-THÖMMES T., SEIFERT F., ZIMMER J., *Relaxation of spin polarized  $^3\text{He}$  by magnetized ferromagnetic contaminants – Part III*, The European Physical Journal D **38**(3), 2006, pp. 445–454.
- [14] NACHER P.J., *Peristaltic compressors suitable for relaxation-free compression of polarized gas*, United State Patent No. US6655931B2, 2003.
- [15] COURTADE E., MARION F., NACHER P.-J., TASTEVIN G., KIERSNOWSKI K., DOHNAŁIK T., *Magnetic field effects on the 1083 nm atomic line of helium – Optical pumping of helium and optical polarisation measurement in high magnetic field*, The European Physical Journal D **21**(1), 2002, pp. 25–55.
- [16] TALBOT C., BATZ M., NACHER P.-J., TASTEVIN G., *An accurate optical technique for measuring the nuclear polarisation of  $^3\text{He}$  gas*, Journal of Physics: Conference Series **294**, 2011, article 012008.
- [17] SUCHANEK M., CIESLAR K., PALASZ T., SUCHANEK K., DOHNAŁIK T., OLEJNICZAK Z., *Magnetic resonance imaging at low magnetic field using hyperpolarized  $^3\text{He}$  gas*, Acta Physica Polonica A **107**(3), 2005, pp. 491–506.
- [18] VIGNAUD A., *Influence de l'intensité du champ magnétique sur l'imagerie RMN des poumons à l'aide d'hélium-3 hyperpolarisé*, Dissertation to get the grade of Docteur en science de l'université Paris XI, Orsay, 2003, p. 85, available online: <http://tel.archives-ouvertes.fr/tel-00003668/en/>.
- [19] SAAM B., HAPPER W., MIDDLETON H., *Nuclear relaxation of  $^3\text{He}$  in the presence of  $\text{O}_2$* , Physical Review A **52**(1), 1995, pp. 862–865.
- [20] NIKIEL A., PALASZ T., SUCHANEK M., ABBOD M., SINATRA A., OLEJNICZAK Z., DOHNAŁIK T., TASTEVIN G., NACHER P.-J., *Metastability exchange optical pumping of  $^3\text{He}$  at high pressure and high magnetic field for medical applications*, The European Physical Journal Special Topics **144**, 2007, pp. 255–263.
- [21] DOHNAŁIK T., NIKIEL A., PALASZ T., SUCHANEK M., COLLIER G., GRENCZUK M., GŁOWACZ B., OLEJNICZAK Z., *Optimization of the pumping laser beam spatial profile in the MEOP experiment performed at elevated  $^3\text{He}$  pressures*, The European Physical Journal – Applied Physics, (in press).
- [22] LEE R.F., JOHNSON G., GROSSMAN R.I., STOECKEL B., TRAMPPEL R., MCGUINNESS G., *Advantages of parallel imaging in conjunction with hyperpolarized helium – A new approach to MRI of the lung*, Magnetic Resonance in Medicine **55**(5), 2006, pp. 1132–1141.
- [23] COLLIER G., NIKIEL G., PALASZ T., SUCHANEK M., GŁOWACZ B., WOJNA A., OLEJNICZAK Z., DOHNAŁIK T., *Metastability exchange optical pumping of  $^3\text{He}$  at 1.5 T for an in-situ polariser*, Poster presented in JCNS Workshop on Modern Trends in Production and Applications of Polarized  $^3\text{He}$ , Munich, 2010, available online: <http://flux.if.uj.edu.pl/posters/Munich2010.pdf>.